Visual phenotyping analysis of *Pcdh18* knockout mice and identification of an association with eye disease

Haesol Shin

Department of Medicine

The Graduate School, Yonsei University

Visual phenotyping analysis of *Pcdh18* knockout mice and identification of an association with eye disease

Directed by Professor Kyoung Yul Seo

The Master's Thesis
submitted to the Department of Medicine,
the Graduate School of Yonsei University
in partial fulfillment of the requirements for the degree
of Master of Medical Science

Haesol Shin

June 2021

This certifies that the Master's Thesis of
Haesol Shin is approved.

Thesis Supervisor : Kyoung Yul Seo

Thesis Committee Member#1 : Ki Taek Nam

Thesis Committee Member#2 : Hosung Jung

The Graduate School
Yonsei University

June 2021

ACKNOWLEDGEMENTS

First of all, I appreciate my thesis supervisor, Professor Kyoung Yul Seo for providing me such inspiring advice and support for preparing this thesis even when he was busy. I also appreciate Professor Ki Taek Nam and Professor Hosung Jung, who gave me valuable advice and encouragement. I would like to thank all of my lab members, Soo Jung Han, Jiyeon Kim, and Munkhdelger Jamiyansharav for all the support that I received everyday. I was also grateful to work with members of KMPC, Dr. Kim, Dr. Min, Dr. Ohk, Yejin Cho, Bora Kim, and Chae-Eun Moon. They gave me kind help and warm support.

Many thanks to my friends who always made me laugh and gave me strength during difficult times, Dabin, Jimin, Raewon, Heeyeon, Myoung joo, Myoung eun and Shinhye. Finally, I would like to express my deepest appreciation to my family. My parents always supported me with prayers and my older sister has always put family first even when she was in Paris. Special thanks to Bbaeggom, who gives me energy through just being existence himself. Their love and encouragement made me to be successful in whatever I pursued. Without help from all these people I mentioned above, my study could not have been impossible. I hereby once again thank everyone for their love in my thesis.

Haesol Shin

<TABLE OF CONTENTS>

ABSTRACT ·····1

I. INTRODUCTION ·····3
II. MATERIALS AND METHODS ·····5
1. Mice ·····5
2. Fundus Photography and Angiography ·····5
3. Optical Coherence Tomography ·····6
4. Electroretinography ·····6
5. Optokinetic Nystagmus ·····7
6. Tonometry ·····8
7. Histology ·····8
8. Statistical Analysis ·····9
III. RESULTS ·····10
1. Preparation of *Pcdh18* knockout mice ·····10
2. Visual phenotyping analysis of *Pcdh18* knockout mice ·····12
3. Confirmation of association between phenotype and eyedisease in *Pcdh18* knockout mouse ·····24
IV. DISCUSSION ·····28
V. CONCLUSION ·····31

REFERENCES ·····32
ABSTRACT(IN KOREAN) ·····34

LIST OF FIGURES

Figure 1. Confirmation of *Pcdh18* deletion in mice ····· 11
Figure 2. Fundus photography of control mice and *Pcdh18* knockout mice. ····· 13
Figure 3. Occurrence of an aberrant mass. ····· 15
Figure 4. Representative of optical coherence tomography (OCT) image of the retina. ····· 17
Figure 5. Comparison of retinal thickness between the control and *Pcdh18* KO groups. ····· 19
Figure 6. Analysis of the anterior segment morphology. ····· 20
Figure 7. Comparison of Visual acuity, Intraocular pressure and retinal function between the control and *Pcdh18* KO group. ····· 22
Figure 8. Remaining of the blood vessels connected to the aberrant mass. ····· 25
Figure 9. Persistent retrolental masses originate from the primary vitreous at embryonic stage and postnatal 5 ····· 27

ABSTRACT

Visual phenotyping analysis of *Pcdh18* knockout mice and identification of an association with eye disease

Haesol Shin

Department of Medicine
The Graduate School, Yonsei University

(Directed by Professor Kyoung Yul Seo)

Humans and mice have 99% identical genes. Therefore, many studies are currently actively researching gene function using genetically modified mice, and through this research, a gene whose function is not known may be identified a gene that causes a specific disease. My research began with this same purpose. The subject of this study, the *Pcdh18* gene, is not as well-known as other protocadherins. In particular, the eyes play an important role in our bodies because humans receive more than 70% of external information through vision, and the relationship between these eyes and *Pcdh18* gene has not been elucidated.

I performed a visual phenotyping analysis using mice with a deletion of the *Pcdh18* gene. In the eyes of most of the *Pcdh18* gene-deficient mice, cell masses that must be eliminated in the developmental stage were present in the vitreous body between the lens and the retina. There was no effect on the structure of the visual organs, such as the cornea, retina and lens, or the function of the optic cells. However, this material obstructed the visual field and the results of a visual acuity test showed decreased visual acuity in knockout (KO) mice compared with those in the control group.

I investigated which eye diseases were most similar to existing visual disorders, and “primary vitreous hyperplasia (PHPV)” showed the most similar

pattern. Primary vitreous proliferation refers to a disease in which the primary vitreous body and blood vessels contained therein, which are lost during the development stage of the eye, do not disappear and remain in the form of a cell mass.

I performed an experiment to evaluate the association between the *Pcdh18* gene and PHPV. First, angiography confirmed that blood vessels that should have disappeared remained present near the cell mass visible in the eyes of *Pcdh18* KO mice. In addition, histopathological analysis confirmed that the normal primary vitreous body remained on day 18.5 of the embryonic stage only after regression occurred on approximately day 15.5th of the embryonic stage.

Based on these experimental results, I proposed that the *Pcdh18* gene is one of the causative genes of PHPV, which causes visual disease, and revealed that the *Pcdh18* gene plays an important role in the early ocular development process. In addition, further in-depth study may suggest a clearer basis for the fact that the *Pcdh18* gene can acts as a tumor suppressor gene.

Key words : *Pcdh18* gene, vision phenotyping, eye disease

Visual phenotyping analysis of *Pcdh18* knockout mouse and identification of an association with eye disease

Haesol Shin

Department of Medicine
The Graduate School, Yonsei University

(Directed by Professor Kyoung Yul Seo)

I. INTRODUCTION

PCDH18, encoded by the *Pcdh18* gene, belongs to the protocadherin (PCDH) group among the subfamily of cadherins, a large family of cell adhesion molecules, and is a calcium-dependent adhesion protein. The PCDH group is divided into clustered and nonclustered PCDHs according to genomic structure, and Pcdh18 belongs to nonclustered PCDHs. Nonclustered PCDHs are mainly expressed in the nervous system, and that various neuropsychiatric disorders occur when a problem occurs with these proteins[1]. Other studies have suggested the possibility of *PCDH18* as a candidate gene for intellectual disability[2]. Related clinical diseases are associated with rare immunodeficiency diseases with high mortality rates called patent foramen ovale and hemophagocytic lymphohistiocytosis; however, little is known about their relationship[3]. Recently, the role of *PCDH18* as a biomarker for the diagnosis of colorectal cancer has also been studied[4].

Except for these, there are fewer accurate molecular biological studies about PCDH18 than there are about other nonclustered PCDHs. The most famous nonclustered PCDH gene is *PCDH15*. Mutations in *PCDH15* are known to cause Usher syndrome, which is characterized by congenital hearing

loss and visual impairment due to retinal pigment degeneration[5]. Studies related to the *PCDH18* gene and the eye have confirmed the expression of the *Pcdh18* gene in the neural tube, central nervous system (CNS), and eyes of zebra fish embryos. In particular, regarding the structure of the eye, research results have confirmed the expression of *Pcdh18* in retina and optic nerve studies[6]. In addition, weak expression was found in some of the retinal layers of ferret embryos[7]. However, there are currently no studies of the relationship of the *PCDH18* gene to vision in mice or in humans.

Therefore, I first studied whether the *Pcdh18* gene is related to vision by a visual phenotypic analysis of mice with a *Pcdh18* gene defect. Based on the results of this phenotypic analysis, the primary vitreous and associated blood vessels (hyaloid), which is lost during the process of eye development, were studied[8]. The hyaloid vascular system (HVS) was not lost, and I attempted to clarify its association with the remaining visual disease. In this disease, a family history has been found, and the symptoms are often caused by genetic factors[9]; therefore, I also tried to clarify that *Pcdh18* is one of the causative genes.

II. MATERIALS AND METHODS

1. Mice

The mice used in this study were from the Knockout Mouse Project (KOMP, University of California, Davis). A detailed description of the mouse line is described in the Results section. Mice were genotyped using the following 4 PCR primers: Reg-LacF (5'-ACT TGC TTT AAA AAA CCT CCC ACA-3'), Reg-Pcdh18-R (5'-GGT CTA CTT CCG TCC TCC ATT TTG C-3'), Reg-Pcdh18-wtF (5'-TTC TCA GTC ATC AAG GGT GAG AGG C-3'), and Reg-Pcdh18-wtR (5'-GCT AGC AGA ATA GTT GCT TCC AGG C-3'). The wild-type (WT) allele was amplified by Reg-Pcdh18-wtF and Reg-Pcdh18-wtR a PCR product of 239 base pairs. The knockout (KO) allele was amplified by Reg-LacF and Reg-Pcdh18-R, yielding a PCR product of 910 base pairs. The timing of embryonic development was determined by presence of a vaginal plug the morning after mating (E0.5). Embryos for analysis were generated by mating male and female mice heterozygous for a *Pcdh18* KO allele. All mice were handled in strict accordance with the guidelines for the Care and Use of Laboratory Animals of Yonsei University College of Medicine, and the study was performed in accordance with the Yonsei Medical Center Animal Research Guidelines, which adhere to the standards articulated in the Association for Assessment and Accreditation of Laboratory Animal Care International (AAALAC) guidelines.

2. Fundus imaging and angiography

The mice were anesthetized with an intraperitoneal (i.p.) injection of tiletamine and zolazepam (30 mg/kg of body weight) and xylazine (10 mg/kg

of body weight). Pupils were dilated with 0.5% tropicamide and 0.5% phenylephrine mixed eye drops (Mydrin-P, Santen Pharmaceutical Co, Ltd.,). Fundus photographs were taken with Micron IV (Phoenix Research Laboratories, Plesanton, CA, USA), with a wavelength range between 450 and 650 nm; the resultant images were stored in Micron IV StreamPix software (Norpix, Inc., Montreal, QC, Canada.). The mice were then administered i.p. injections of fluorescein (AK-FLUOR 10%, Sigma Pharmaceuticals, North Liberty, IA, USA), and the retinal vasculature was evaluated with blue light illumination after 5 min when all the vessels were filled.

3. Optical coherence tomography (OCT)

After anesthesia, the pupils were dilated with 0.5% tropicamide and 0.5% phenylephrine mixed eye drops (Mydrin-P, Santen Pharmaceutical Co, Ltd., Osaka, Japan). OCT scans were taken using Micron® IV (Phoenix Research Labs, Pleasanton, CA, USA). The cornea was lubricated with 2.5% hypromellose (Goniovisc®, Hub Pharmaceuticals LCC, CA, USA), and the mice were placed collaterally in front of the OCT camera on the right side of a platform that was fixed in front of the OCT lens. We then focused on the retina and obtained fundus photographs and OCT scans. The retinal thickness was measured using the InSight—Animal OCT Segmentation Software (Phoenix Research Labs, CA, USA).

4. Electroretinography (ERG)

ERG recordings were performed using Micron Ganzfeld ERG (Phoenix Research Labs, Pleasanton CA, USA). Mice were dark-adapted

overnight at least 12 hours before the experiment for scotopic testing (rod cell response). After anesthesia, the pupils were dilated as previously described. Once the pupils were adequately dilated, we applied 2.5% hypromellose (Goniovisc®) and inserted the electrodes. ERGs were recorded according to the standard protocol provided with the manual. Scotopic ERGs were obtained in response to increasing flash intensities ranging from -1.7 log cd·s/m^2 to 1.9 log cd·s/m^2. Photopic ERGs were obtained in response to increasing flash intensities ranging from -0.5 log cd·s/m^2 to 4.1 log cd·s/m^2. Ten responses to light stimulation were averaged. The a-wave (as a measure of photoreceptor function), b-wave (as a measure of bipolar cell function), amplitude, and implicit times of rod and cone responses were determined.

5. Optokinetic nystagmus (OKN)

Spatial frequency thresholds (i.e., visual acuity) were assessed by optokinetic nystagmus (OKN) using a virtual optokinetic system (OptoMotry, Cerebral Mechanics, Medicine Hat, Alberta, Canada). One to three vertical sine-wave gratings moving at 12°/s, drifting either to the left or right, were projected on four surrounding monitors, while an unrestrained mouse stood on an elevated platform in the center of an arena. A video camera was placed on the ceiling of the device and transmitted the image to the connected computer. Clockwise movement drove the tracking through the left eye, while counterclockwise motion drove it through the right eye. The experimenter judged whether the mouse made slow tracking movements with its head and body to follow the drifting grating. Major repositioning of the head and grooming movements were ignored, and the trial was restarted if the presence or absence of tracking was unclear. The maximum spatial frequency capable of driving the head tracking was determined.

6. Tonometry

Mice were anesthetized with an i.p. injection of xylazine (10 mg/kg; Rompun® , Bayer Animal Health) and zolazepam and tiletamine (30 mg/kg; Zoletil 50® , Vibrac, Carros, France). Intraocular pressure (IOP) was measured using a rebound tonometer (Icare® TONOLAB tonometer, Colonial Medical Supply, Franconia, NH, USA). IOP measurements were taken according to the manufacturer's instructions. One trial result was recorded after six consecutive measurements, and the mean of consecutive trials was used for analyses.

7. Histology

For histologic examination, embryo heads (embryonic day 14.5 [E14.5]) were fixed in 4% formaldehyde. Dissected eyes (embryonic day 18.5 [E18.5], postnatal day 5, adult) were fixed in 4% Davidson's solution for 24 h with gentle shaking. The eyes were fixed in 4% formaldehyde, 5% acetic acid, and 3% sucrose at 48℃ overnight. Fixed samples were embedded in paraffin and cut into 4-μm sections using a microtome (RM2335, Leica, Wetzlar, Germany). Hematoxylin and eosin (H&E) staining was performed the day after sectioning. Sections were stained with H&E according to standard procedure.

8. Statistical analysis

Statistical analysis were performed with GraphPad Prism v.5 software (GraphPad, San Diego, CA, USA). Comparison between groups was performed with the Mann-Whitney *U* test and unpaired t-test. The result of experiments were presented as mean ±standard error of mean. $P<0.05$ was considered significant.

III. RESULTS

1. Preparation of *Pcdh18* knockout mice

Pcdh18 KO mice were generated by in vitro fertilization using sperm from the *Pcdh18*$^{tm1.1(KOMP)\ Vlcg}$ line (KOMP, University of California, Davis), which lacks part of exons 1 and 4 of the *Pcdh18* gene (Figure 1A). In the Velocigene KOMP project, a targeted deletion was created via homologous recombination using a ZEN-UB1 cassette containing a lacZ reporter and a loxP-flanked selection marker. The targeted allele in these mice was designated tm1. Mice that contained the tm1 allele were bred to Cre-expressing mice, resulting in the removal of beta-actin promoter and the Neomycin gene that it activates. The resulting mice carried the tm1.1 allele and were used for this study. Heterozygous mice (*Pcdh18*+/-) were intercrossed to obtain the *Pcdh18* KO mice used for vision phenotyping. *Pcdh18* gene deletion was confirmed by PCR on genomic DNA (Figure 1B). The top bands (910 bp) correspond to the KO allele (*Pcdh18*-), and the bottom bands (239 bp) corresponds to the WT allele (*Pcdh18*+).

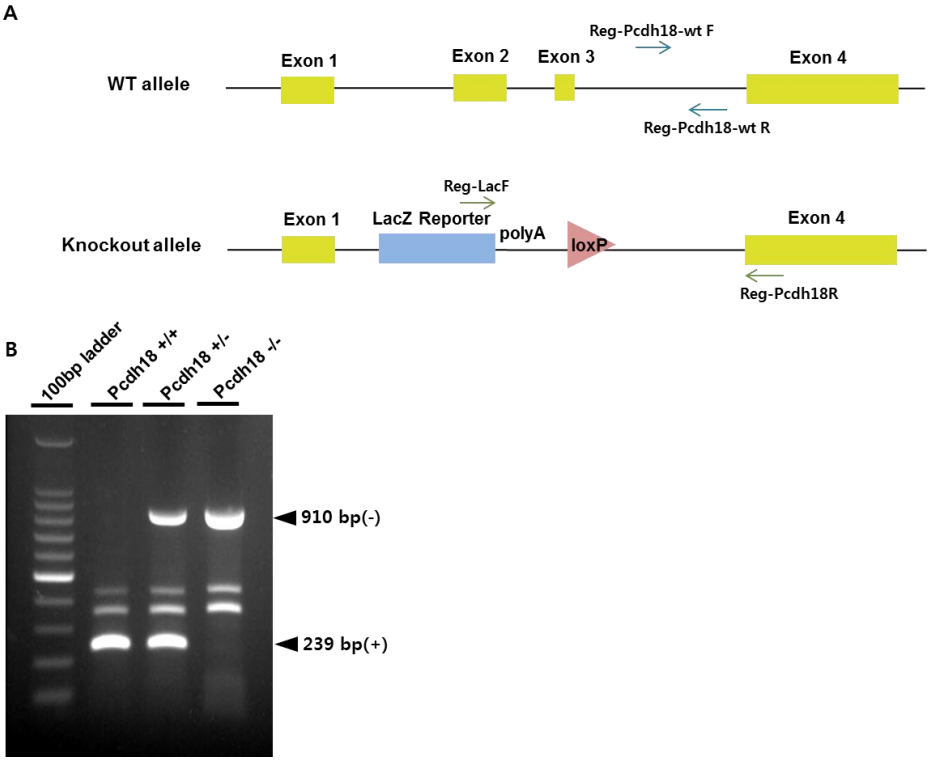

Figure 1. Confirmation of *Pcdh18* deletion in mice. (A) Schematic representation of the *Pcdh18* KO strategy. (B) Genotyping of the WT and mutant allele was performed by PCR on genomic DNA samples from tail biopsies. A representative image from PCR amplifications obtained by the combination of primers using primers distinguish the mutant (upper bands, 910 bp) and WT (lower bands, 239 bp).

2. Visual phenotyping analysis of *Pcdh18* KO mice

A visual phenotypic analysis was performed to determine whether there were any abnormalities in the visual structure and function of *Pcdh18* KO mice. I found interesting results. Both the *Pcdh18*+/+ genotype group and the *Pcdh18*+/- genotype group showed fundus results similar to normal mice. I evaluated these two genotypes by integrating them into a control group (Figure 2A-C). However, yellow irregular masses were found in almost all fundus photographs of mice in the *Pcdh18*-/- genotype group. As can be seen from the fundus photographs taken each week of the *Pcdh18*-/- group, these aberrant masses did not increase in size as the mice aged (Figure 2 D-I).

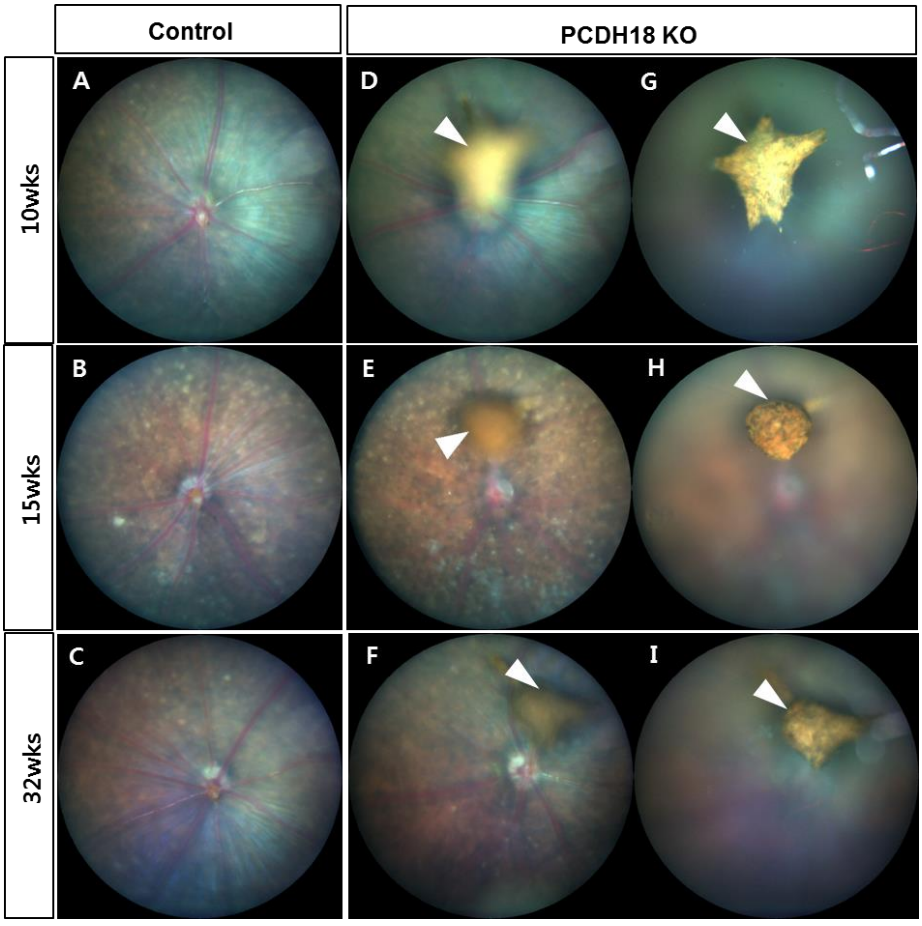

Figure 2. Fundus photography of control mice and *Pcdh18* KO mice.

(A-C) Fundus photographs of control mice at 10, 15, and 32 weeks. (D-F) Fundus photographs of *Pcdh18-/-* mice at 10, 15, and 32 weeks. Yellow irregular tissue (white arrowhead) was found in *Pcdh18-/-* mice. (G-I) Fundus image focusing on the yellow irregular tissue (white arrowhead).

When analyzing the occurrence of an aberrant mass, almost all control mice did not have aberrant masses, while almost all *Pcdh18*-/- mice were observed to have aberrant masses. Figure 3 shows the incidence of an aberrant mass in the groups by age. A 10, 30, and 40 weeks of age, the prevalence of an aberrant mass 0% in the control group and 100% in the *Pcdh18* KO group. In 15-week-old mice, an aberrant mass was observed in 1 of hetero genotype out of 4 eyes in the control group, resulting in a prevalence of 25%, and the prevalence was 100% in the *Pcdh18* KO group. At 20 weeks of age, 0% of the control group had an aberrant mass, and 66.7% of the *Pcdh18* KO group had aberrant masses. Overall, in the control group, aberrant mass was found in 1 eye out of a total of 16 eyes, resulting in a prevalence of 6.25%, and in the *Pcdh18*-/- group, an aberrant mass was found in 18 eyes out of a total of 20 eyes, resulting in a prevalence of 90% (Figure 3).

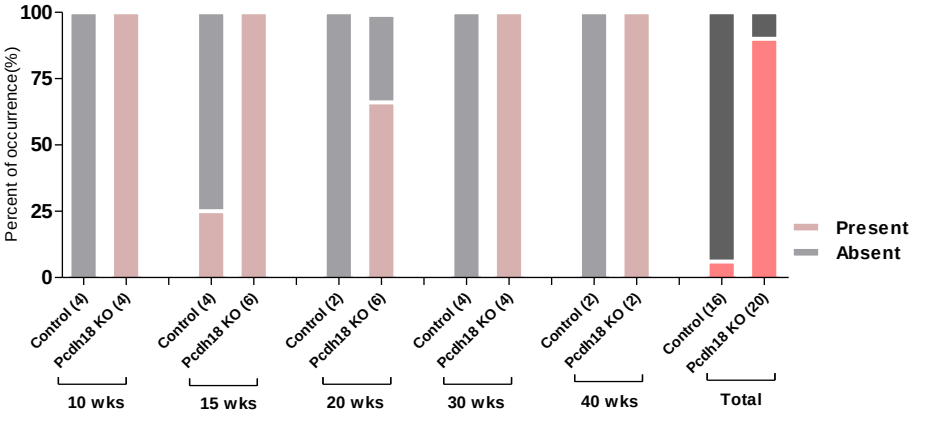

Figure 3. Occurrence of an aberrant mass. Graph of the presence of aberrant mass in the control group and *Pchd18* KO group. The occurrence was calculated by dividing the incidence of an aberrant mass per eye at 10 weeks, 15 weeks, 20 weeks, 30 weeks, and 40 weeks. The number in parentheses indicates the number of eyes.

I performed OCT measurements to evaluate abnormalities in the retinas of eyes with aberrant masses (Figure 4). In the control group, the normal retinal layer including the optic disc was visualized through horizontal and vertical OCT scanning. However, OCT analysis of the eyes of *Pcdh18-/-* mice revealed that the presence of an aberrant mass was sufficient to block the path of infrared light penetration for OCT signal acquisition, as shown in Figure 4H. The OCT results of another *Pcdh18* KO mouse (Figure 4I, I') show that part of the retina is not visible in Figure 4H due to the shadow caused by the mass, but the retinal structure is normal.

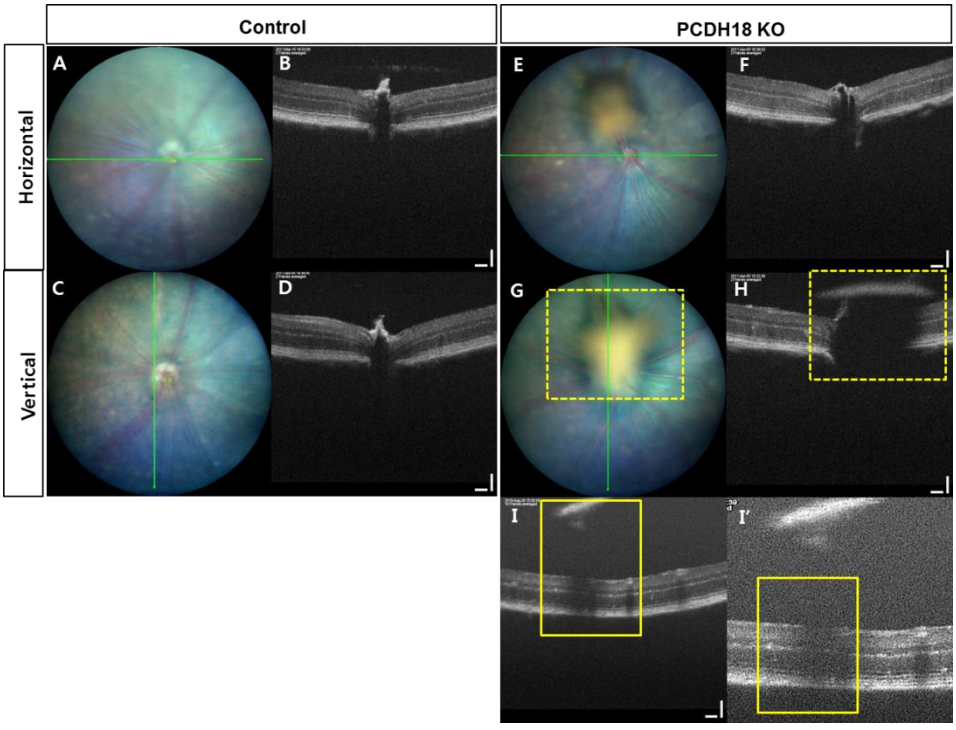

Figure 4. Representative OCT images of the retina. (A,C) Normal fundus image and (B,D) normal retinal OCT scan in the control group. (E,G) Fundus image and (F,H) retinal OCT scan in the *Pcdh18* KO group. The *Pcdh18* KO group showed the presence of asteroid-like structures above the retinal layers. These masses were able to block the light path through the retina; thus, the retina generated a shadow (yellow dashed box). (I) Retinal OCT image of another *Pcdh18* KO mouse. (I') Detailed image of the solid yellow box shown in (I). Scale bar: 100 μm.

I analyzed the retinal thickness to determine whether the thickness in the *Pcdh18* KO group was different from that in the control group. The retina was divided into three parts: 1) from the retinal nerve fiber layer (RNFL) to the inner nuclear layer (INL); 2) from the outer plexiform layer (OPL) to the outer nuclear layer (ONL); and 3) from the inner segment (IS) and outer segment (OS) to the retinal pigment epithelium (RPE) (Figure 5A). OCT retinal layer depth analysis showed that there were no statistically significant differences between the *Pcdh18* KO group and the control group in all three compartments and the total retina (Figure 5B-E).

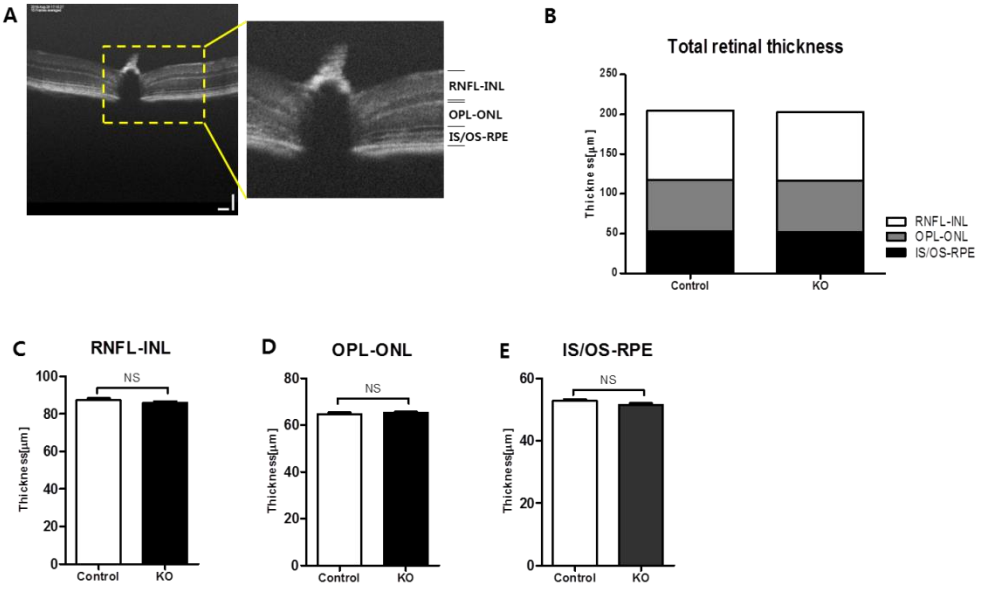

Figure 5. Comparison of retinal thickness between the control and *Pcdh18* KO groups. (A) Representative image of the distribution of the retinal layer where the thickness was analyzed. (B) Comparison of the total retinal thickness. (C-E) Graphs divided into three parts and analyzed for comparison. There were no differences in the thicknesses of all three layers between the control and *Pcdh18* KO groups. RNFL, retinal nerve fiber layer; INL, inner nuclear layer; OPL, outer plexiform layer; ONL, outer nuclear layer; IS/OS, inner and outer segments; RPE, retinal pigment epithelium. Scale bars: 100 μm. NS, not significant. Controls are *Pcdh18*+/+ and *Pcdh18*+/- (n=16 eyes). *Pcdh18* -/- (n=20 eyes).

Next, I analyzed the corneas and lenses of *Pcdh18* KO mice. The cornea was normal in both the control and *Pcdh18* KO groups based on external eye photos (Figure 6 A,B). The corneal thickness and lens morphology were also assessed with OCT (Figure 6 C,D). As a result of the corneal thickness analysis, there were no statistically significant differences between the two groups (Figure 6E). It was confirmed that no structural eye changes occurred due to the deletion of the *Pcdh18* gene in the anterior segment.

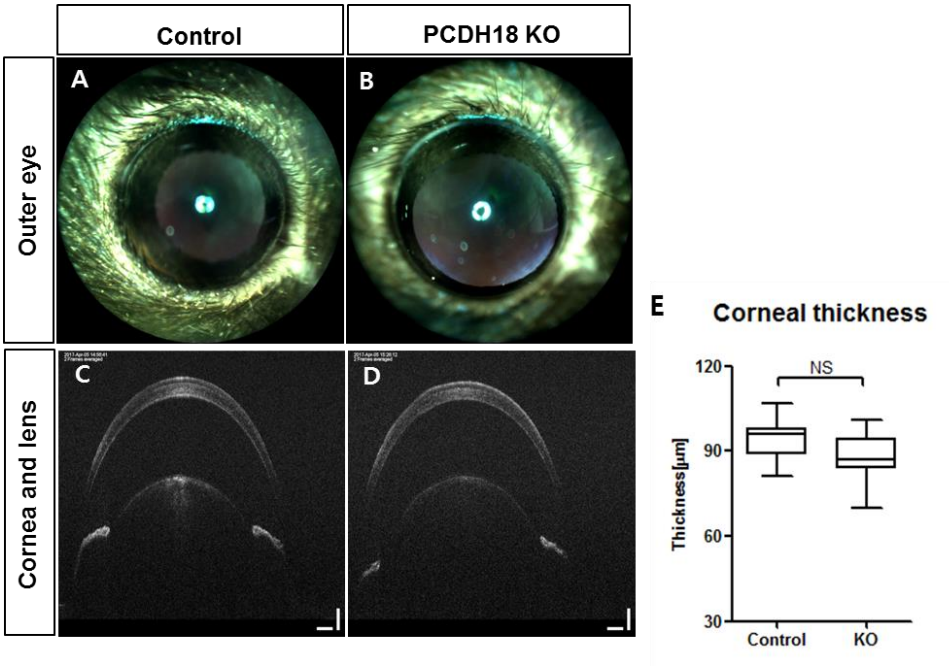

Figure 6. Analysis of the anterior segment morphology. (A,C) Normal outer eye image and normal corneal and lens OCT images from the control group. (B,D) Normal outer eye image and normal corneal and lens images from the *Pcdh18* KO group. (E) Corneal thickness comparison between the two groups. Scale bars: 100 μm. NS, not significant. Controls are *Pcdh18*+/+ and *Pcdh18*+/- (n=16 eyes). *Pcdh18* -/- (n=20 eyes).

Other measurements were also performed to confirm that there was no effect on the function of the eye. First, a visual acuity test was performed, which showed that the *Pcdh18* KO mice had a lower average visual acuity (0.305 c/d) than the control mice (0.360 c/d) (Figure 7A). Second, the IOP test was measured. The average IOP of was 12.05 mmHg and 12.00 mmHg in the control and *Pcdh18* KO groups, respectively. The statistical analysis showed that there were no differences in IOP between the two groups (Figure 7B).

Finally, the function of rod and cone cells was analyzed through ERG. The results of the function tests of rod cells performed after dark adaptation and those of cone cells performed after light adaptation showed no difference between the two groups. The scotopic wave and photopic wave graphs confirmed that there were no differences in the rod and cone cell functions between the control and *Pcdh18* KO groups (Figure 7C, D). Furthermore, there was no difference between the a-wave amplitude, which evaluates photoreceptor cell function, or the b-wave amplitude, which evaluates bipolar cell function. There was also no difference in the reaction rate (Figure 7E,G). However, the amplitude of the *Pcdh18* KO group was higher than that of or similar to that of the control group.

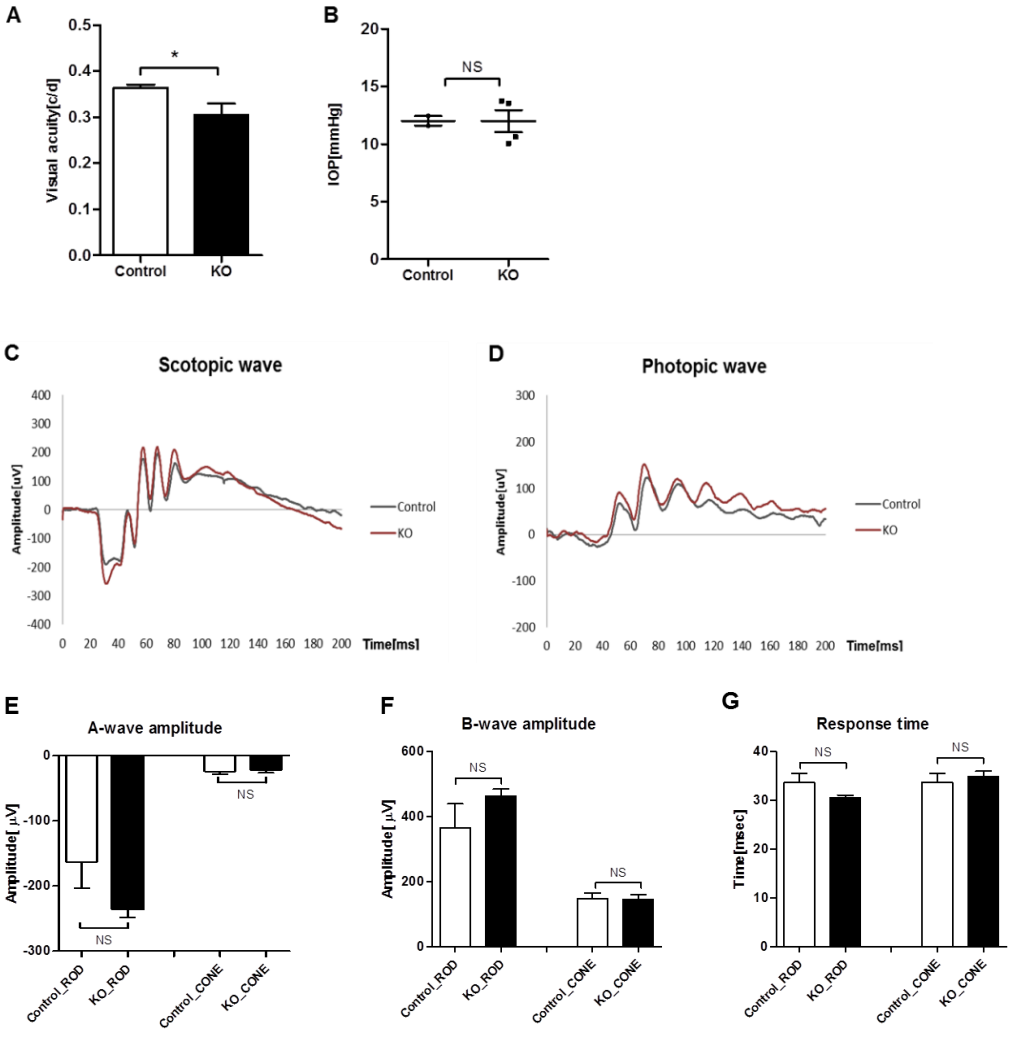

Figure 7. Comparison of Visual acuity, Intraocular pressure and retinal function between the control and *Pcdh18* KO groups. (A) Comparison of visual acuity; *P < 0.05 compared with the control group. Statistical analysis was performed with the Mann-Whitney U test. control group, n=7; *Pcdh18-/-* group, n=7. (B) Comparison of IOP; ns, not significant. Statistical analysis with an unpaired t-test. control group, n=2; *Pcdh18-/-* group, n=4. (C,D) Representative images of scotopic and photopic ERG waves after light exposure. (E-G) Comparison of rod and cone cell function between groups by

ERG amplitude analysis. ns, not significant. Statistical analysis was performed with the Mann-Whitney U test. control group, n=6; *Pcdh18-/-* group, n=8.

3. Confirmation of an association between phenotype and ocular disease in *Pcdh18* KO mice

Through visual phenotypig examination of *Pcdh18* KO mice, I found that there was a mass that should have disappeared in the vitreous of almost all *Pcdh18* KO mice. Then I evaluated what visual disorders this phenotype was associated with. Based on this analysis, the most related disease was selected, and two experiments were conducted to determine if the characteristics of this disease were also seen in *Pcdh18* KO mice.

First, the mice were photographed with fundus fluorescein angiography (FFA) to determine whether blood vessels were present in the mass observed in the vitreous or whether the mass was connected to blood vessels. Two focal planes were used: one view was focused on the retina, and one view was focused on the vitreous and the aberrant mass between the humor and the posterior lens. Nothing was seen when focusing on vitreous in control mice. However, in the FFA image of 15-week-old *Pcdh18* KO mice, there were blood vessels connected to the aberrant mass (Figure 8).

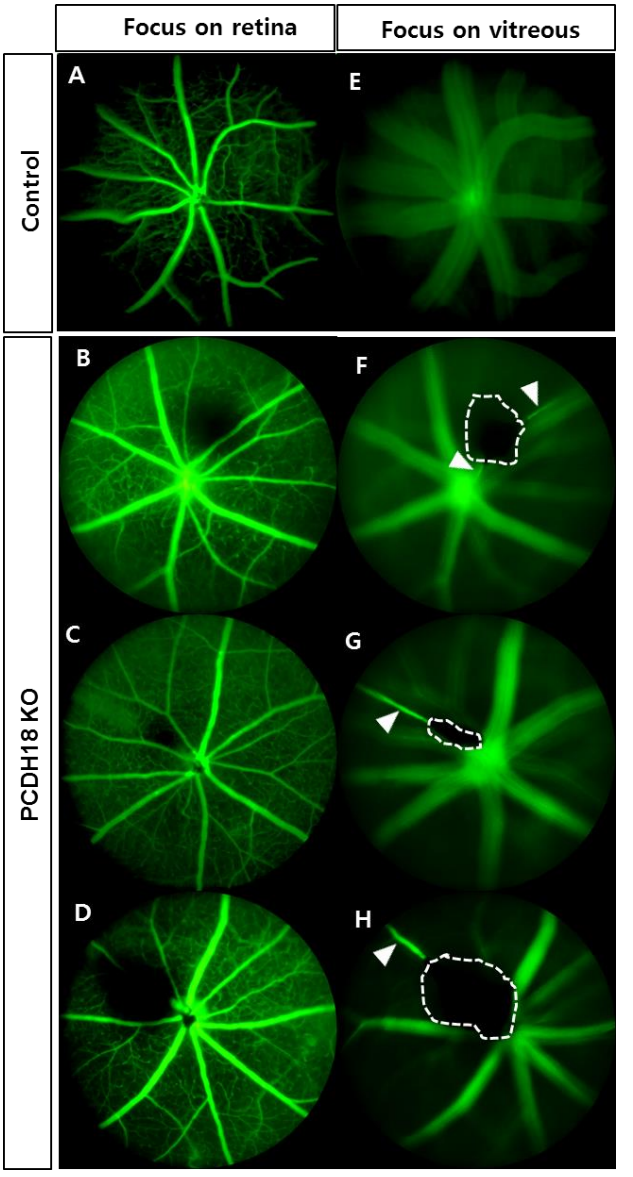

Figure 8. Remaining of the blood vessels connected to the aberrant mass. (A-D) FFA image focused on the retina. A is a picture of the control mouse, and B-D are pictures of *Pcdh18* KO mice. (E-H) FFA image focused on the vitreous. The angiography images of *Pcdh18* KO mice focused on the aberrant mass (white dotted line). Blood vessels connected to the aberrant mass are shown in F-H (white arrowhead).

Next, I investigated associations between *Pcdh18* KO mice and eye diseases by histopathological methods. First, as a result of embryo eye dissection on day E14.5, retrolental primary vitreous cell masses were found in both the control and *Pcdh18* KO groups. The primary vitreous body is a structure that exists temporarily during the embryonic stage and is formed by the capillary network released from the hyaloid artery and fibroblastic cells grown from the periocular mesenchyme (Figure 9A, B).

Therefore, as a result of eye dissection on day E18.5, the retrolental primary vitreous cell masses regressed in the control group, and only acellular secondary vitreous and hyaloid vessels remained. However, in the *Pcdh18* KO group, the primary vitreous regression failed, and the retrolental primary vitreous cell mass was still present (Figure 9C, D).

Similarly, eye dissection in the P5 group showed that the retrolental primary vitreous cell mass still remained only in the eyes of *Pcdh18* KO mice (Figure 9E-G). I also performed serial sections to determine if there was a retrolental mass in the eyes of the control mice on postnatal day 5, but there was no abnormal mass (data not shown). The difference from the embryo stage is that this abnormal cell mass was accompanied by vasculature and pigmented cells. As shown in Figure 9G, the inner retina and abnormal mass were attached, and the retina was not normally generated and folded.

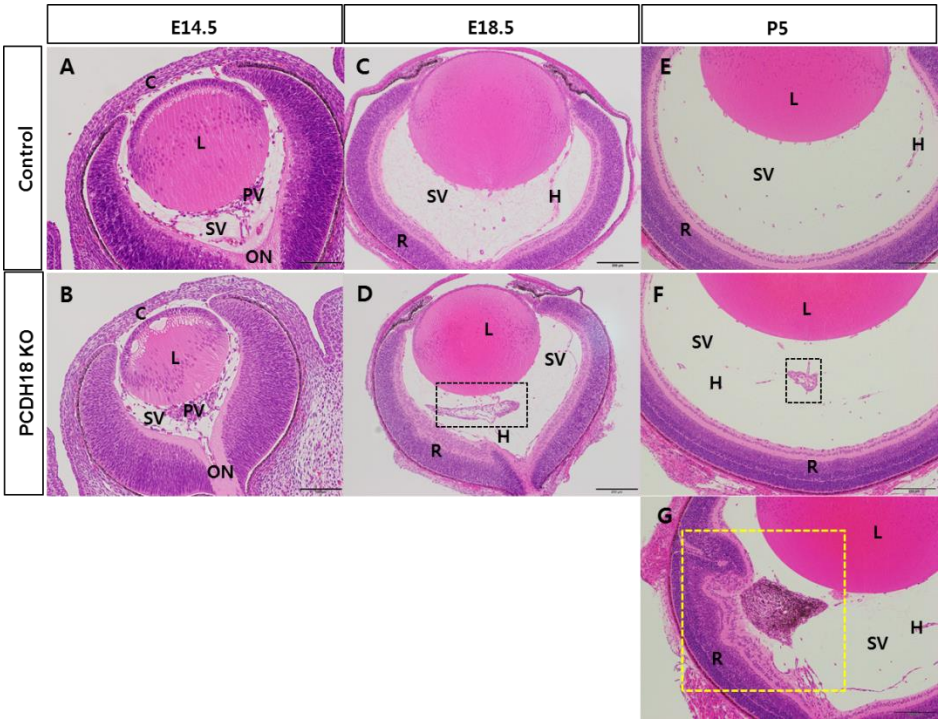

Figure 9. Persistent retrolental masses originate from the primary vitreous at embryonic stage and postnatal 5. (A) Sagittal sections of a mouse head from the control group on day E14.5 . (B) Sagittal sections of a mouse head from the *Pcdh18* KO group on day E14.5. (C) Sagittal sections of a mouse eye from the control group on day E18.5. (D) Sagittal sections of a mouse eye from the *Pcdh18* group on day E18.5. Cell mass presumed to be primary vitreous (black dotted line). (E) Sagittal sections of a mouse eye from the control group on postnatal day 5. (F) Sagittal sections of the right eye from a mouse in the *Pcdh18* KO group on postnatal day 5. Cell mass presumed to be primary vitreous (black dotted line). (G) Sagittal sections of the left eye from a mouse in the *Pcdh18* KO group on postnatal day 5. The retrolental mass in which pigmented cells are observed is attached to the inner retina (yellow dashed box). C, cornea; H, hyaloid vessel; L, lens; ON, optic nerve; R, retina; PV, Primary vitreous; SV, Secondary vitreous; Bar indicates 200 μm.

IV. DISCUSSION

In this study, the *Pcdh18* gene was found to have a function that contributes to ocular development. In 90% of the eyes of *Pcdh18* KO mice, a very rare retrolental mass was found, and the retinal structure and function were not affected. However, visual acuity experiments revealed that this retrolental mass obstructed the visual field; thus, the visual acuity was lower in the *Pcdh18* KO group than in the control group. I investigated this vision phenotype result to determine what ocular disease it might be associated with. It is presumed to be related to persistent hyperplastic primary vitreous (PHPV), a rare congenital developmental malformation of eye.

The primary vitreous is a temporary collection of cells derived from the neural crest and mesoderm, which provide nutrients to early ocular tissue, that contain the vitreous fluid during the early stages of eye development[10]. This is a very important process for the normal formation of the crystalline vitreous in the development of young eyes, and light travels undisturbed to the retina and to yield accurate vision. If the primary vitreous does not disappear when it should be eliminated, PHPV develops. PHPV involves the presence of a hyperplastic mass consisting of pigmented and vascular cells behind the lens[11].

I considered PHPV as an eye disease that could be associated with the *Pcdh18* KO gene and conducted an experiment to identify a link. Fibroblasts form the primary vitreous body and between days E13.5 and E14.5. Then, they are rapidly dispersed, become the secondary vitreous, and are no longer visible by day E15.5. Our experimental results were also consistent with this process. In control mice, the primary vitreous seen on day E14.5 regressed on day E18.5. However, in the *Pcdh18* KO mice, on day E18.5, a densely packed cell mass was found between the retina and the lens. On postnatal 5 day, *Pcdh18* KO mice also showed this mass. The retina and retrolental tissue adjacent to the inner retina were also confirmed. PHPV can be divided into two types,

anterior and posterior, and my findings are consistent with the characteristics of posterior PHPV. Posterior PHPV may be accompanied by severe symptoms such as retinal folding and dysplasia[12].

Second, the hyaloid vascular system that provided nutrients to the eye during the embryonic stage of PHPV must completely regress at the later stage of development, but it fails and the remaining hyaloid vascular system is accompanied by cell mass[11]. Angiography was performed to determine whether the retrolental mass seen in *Pcdh18* KO mice also had accompanying blood vessels. The retrolental mass and vessels were found to be connected. Thus, the formation of a retrolental mass in the eyes of *Pcdh18* KO mice is associated with an eye disease called PHPV.

Few studies have been conducting to evaluate the *Pcdh18* gene and the mouse or human eye. Through a literature review, I also found other associations between *Pcdh18* and PHPV. The *ARF* and *p53* genes, which are widely known as tumor suppressor genes, promote hyaloid vasculature regression[11,13,14]. Both of these genes are involved in the activation of the apoptotic pathway, and apoptosis is part of the pathogenesis of PHPV[15]. PCDH10, which belongs to a PCDH subgroup similar to PCDH18, has also been found to play an important role in apoptosis of tumor cells in various cancers as a tumor suppressor gene[16-18]. PCDH18 is also a potential biomarker of colorectal cancer, and some research results have shown that it may be a tumor suppressor gene. In this study, when PCDH18 was overexpressed, migration and proliferation of colorectal cancer cells were suppressed, and this mechanism was found to be regulated by the Wnt/ß-catenin signaling pathway[4]. In connection with this, the fact that PHPV develops even when there is a problem with the *Fzd4* gene or *Lrp5* gene related to Wnt signaling is an important link for me[15,19-21]. One of the reasons for this is that the molecular interaction networks of *Pcdh18* gene contain the *Ctnnb1* gene that encodes ß-catenin, and one study showed that PHPV develops when a mutation occurs in

this gene[4,22]. According to the abovementioned research results, the *Pcdh18* gene also plays a role as a tumor suppressor gene, and when the *Pcdh18* gene is knocked out, apoptosis does not occur, and cell proliferation and migration increase, leading to eye diseases such as PHPV.

In addition to our research results, we plan to clarify that the *Pcdh18* gene is the causative gene of PHPV through a further study confirming the cellular population of the retrolental masses and the association between *Pcdh18* gene and apoptosis based on the abovementioned research.

V. CONCLUSION

In conclusion, I obtained spatiotemporal data through visual phenotyping and histopathology of *Pcdh18* KO mice and found a possible association with PHPV.

First, through the visual phenotyping of *Pcdh18* KO mice, I found retrolental masses when there was a problem during the eye development stage in the vitreous between the lens and retina. Large pigmented retrolental masses were found in both the postnatal stage as well as in adult mice. This substance obstructed the visual field, and the visual acuity value was lower among affected mice than among those in the control group. Angiography confirmed that blood vessels were connected to the aberrant mass, and through this finding, the first association with PHPV was suggested.

Next, through observation of the embryo stage on days E14.5 and E18.5, the primary vitreous cell mass that should have disappeared on day E15.5 remained on day E18.5 in the case of *Pcdh18* KO mice. Through this, a second connection with PHPV was suggested.

Based on these results, I suggest that *Pcdh18* is also one of the causative genes that induce PHPV. We also revealed that the *Pcdh18* gene plays an important role in the early ocular development process. In addition, I proposed a basis to support further studies of the *Pcdh18* gene as a tumor suppressor gene.

REFERENCES

1. Redies C, Hertel N, Hübner CAJBr. Cadherins and neuropsychiatric disorders. 2012;1470:130-44.

2. Kasnauskiene J, Ciuladaite Z, Preiksaitiene E, Matulevičienė A, Alexandrou A, Koumbaris G, et al. A single gene deletion on 4q28. 3: PCDH18–a new candidate gene for intellectual disability? 2012;55:274-7.

3. Duga B, Czako M, Komlosi K, Hadzsiev K, Torok K, Sumegi K, et al. Deletion of 4q28. 3-31.23 in the background of multiple malformations with pulmonary hypertension. 2014;7:1-6.

4. Zhou D, Tang W, Su G, Cai M, An H-X, Zhang YJSr. PCDH18is frequently inactivated by promoter methylation in colorectal cancer. 2017;7:1-12.

5. Ahmed ZM, Riazuddin S, Bernstein SL, Ahmed Z, Khan S, Griffith AJ, et al. Mutations of the protocadherin gene PCDH15 cause Usher syndrome type 1F. 2001;69:25-34.

6. Kubota F, Murakami T, Tajika Y, Yorifuji HJIJoDB. Expression of protocadherin 18 in the CNS and pharyngeal arches of zebrafish embryos. 2004;52:397-405.

7. Etzrodt J, Krishna-K K, Redies CJBn. Expression of classic cadherins and δ-protocadherins in the developing ferret retina. 2009;10:1-13.

8. Saint-Geniez M, D'Amore PAJTIjodb. Development and pathology of the hyaloid, choroidal and retinal vasculature. 2004.

9. Shastry BSJC, ophthalmology e. Persistent hyperplastic primary vitreous: congenital malformation of the eye. 2009;37:884-90.

10. Son AI, Sheleg M, Cooper MA, Sun Y, Kleiman NJ, Zhou RJIo, et al. Formation of persistent hyperplastic primary vitreous in ephrin-A5−/− mice. 2014;55:1594-606.

11. Martin AC, Thornton JD, Liu J, Wang X, Zuo J, Jablonski MM, et al. Pathogenesis of persistent hyperplastic primary vitreous in mice lacking the arf tumor suppressor gene. 2004;45:3387-96.

12. Ruiz A, Mark M, Jacobs H, Klopfenstein M, Hu J, Lloyd M, et al. Retinoid content, visual responses, and ocular morphology are

compromised in the retinas of mice lacking the retinol-binding protein receptor, STRA6. 2012;53:3027-39.

13. McKeller RN, Fowler JL, Cunningham JJ, Warner N, Smeyne RJ, Zindy F, et al. The Arf tumor suppressor gene promotes hyaloid vascular regression during mouse eye development. 2002;99:3848-53.

14. Skapek S, McKeller R, Fowler J, Martin A, Valencia A, Wei TJIO, et al. The ARF Tumor Suppressor Is Essential for Vitreous Maturation and Hyaloid Vascular Regression. 2003;44:430-.

15. Wang Z, Liu C-H, Huang S, Chen JJPir, research e. Wnt Signaling in vascular eye diseases. 2019;70:110-33.

16. Wolverton T, Lalande MJG. Identification and characterization of three members of a novel subclass of protocadherins. 2001;76:66-72.

17. Li Z, Yang Z, Peng X, Li Y, Liu Q, Chen JJMmr. Nuclear factor-κB is involved in the protocadherin-10-mediated pro-apoptotic effect in multiple myeloma. 2014;10:832-8.

18. Mah KM, Weiner JA. Regulation of Wnt signaling by protocadherins. Seminars in cell & developmental biology: Elsevier; 2017. p.158-71.

19. Robitaille JM, Wallace K, Zheng B, Beis MJ, Samuels M, Hoskin-Mott A, et al. Phenotypic overlap of familial exudative vitreoretinopathy (FEVR) with persistent fetal vasculature (PFV) caused by FZD4 mutations in two distinct pedigrees. 2009;30:23-30.

20. Kato M, Patel MS, Levasseur R, Lobov I, Chang BH-J, Glass DA, et al. Cbfa1-independent decrease in osteoblast proliferation, osteopenia, and persistent embryonic eye vascularization in mice deficient in Lrp5, a Wnt coreceptor. 2002;157:303-14.

21. Gong Y, Slee RB, Fukai N, Rawadi G, Roman-Roman S, Reginato AM, et al. LDL receptor-related protein 5 (LRP5) affects bone accrual and eye development. 2001;107:513-23.

22. LM ZG, SC CM, GJ VR, JD BA, JH MVJAdlSEdO. CTNNB1 gene mutation associated with neurodevelopmental disorder, microcephaly, and persistence of bilateral hyperplastic primary vítreous: a case report and literature review. 2021.

ABSTRACT(IN KOREAN)

Pcdh18 유전자 결손 마우스의 시각 표현형 분석 및 시각기 질환과의 연관성 규명

<지도교수 서 경 률>

연세대학교 대학원 의학과

신 해 솔

유전자 기능 해석에 대한 관심이 증대되고 있는 요즘, 사람과 99%의 유전자 일치율을 보이는 동물인 마우스를 이용한 연구는 전 세계적으로 활발히 진행 중이다. 본 연구에서도 *Pcdh18* 유전자 결손 마우스를 이용하여 시각기 에서의 *Pcdh18* 유전자 기능을 확인 하고자 하였다.

이를 위해 먼저 시각표현형분석을 진행한 결과 각막, 망막, 수정체 등의 시각기 구조와 시세포 기능 그리고 안압 에는 이상이 없었으나 90%이상의 *Pcdh18* 유전자 결손 마우스의 유리체 내에 비정상적으로 존재하는 별모양의(asteroid-like) 물질이 발견되었고 정상 마우스에 비해 감소된 시력 값을 보였다. 이러한 결과는 초기 눈 발생단계에서 소실되어야 하는 일차유리체와 혈관들이 퇴행되지 못하여 세포덩어리 형태로 유리체 내에 남아있고 심한 경우에는 실명에 이르게 되는 선천성 희귀 시각질환인 '일차유리체증식증 (PHPV)'과 유사하였다.

이 후, *Pcdh18* 유전자와 PHPV와의 연관성 확인을 위한 실험을 진행하였다. 혈관 조영술을 이용하여 유리체 내의 이상물질에 연결되어 있는 퇴행되지 않은 혈관을 확인하였고, 배아 단계 15.5일경 퇴행되어야 정상인 일차 유리체가 *Pcdh18* 유전자 결손 마우스의 배아 단계 18.5일에도 남아 있음이 조직병리분석 결과를 통해 확인되었다.

본 연구에서는 위 결과들을 바탕으로 *Pcdh18* 유전자가 초기 눈 발생 과정 중 일차유리체의 퇴행 과정을 조절하는 중요한 역할을 하고, PHPV를 유발하는 원인 유전자 중 하나임을 밝혔다.

핵심되는 말 : *Pcdh18* 유전자, 시각표현형분석, 시각기질환